Forensic Investigation of the Deepwater Horizon Blowout Preventer

Shane R. Finneran, Barbara N. Padgett, Brandon C. Rollins, and Neil G. Thompson

Det Norske Veritas (U.S.A.), Inc.

Abstract: *The DWH oil spill was the largest offshore oil spill in United States history. A Joint Investigation Team (JIT) of the Departments of the Interior (DOI) and Homeland Security (DHS) was charged with investigating the explosion, loss of life, and blowout associated with the DWH drilling rig. Det Norske Veritas (U.S.A.), Inc. (DNV GL) was retained to perform a forensic investigation into the technical root causes of the inability of the blowout preventer to kill the well. This paper describes the overall investigative process and the specific role that finite element analysis and simulation played in the forensic investigation.*

Keywords: *Blowout Preventer, Buckling, Damage Modeling, Deepwater Drilling, Failure Analysis, Forensic Investigation, Pipeline, Shear Damage, Wellbore.*

1. Introduction to the Investigation

On the evening of April 20, 2010, control of an exploratory well at the Macando Prospect was lost, allowing hydrocarbons to enter the drilling riser and reach the Deepwater Horizon (DWH) drilling rig. The subsequent explosions and fires onboard resulted in the rig sinking on April 22, 2010 and the loss of eleven lives. Hydrocarbons continued to flow from the well until September 19, 2010, when a relief well was completed.

The DWH was a semi-submersible, dynamically positioned, mobile offshore drilling unit designed to operate in waters up to 8,000 feet deep with an ability to drill to maximum depth of 30,000 feet. The BOP, had been in use on the DWH since the commissioning of the rig in 2001. The BOP sits on the sea floor, directly above the wellhead and is used in normal drilling function as well as the means to seal a well in the instance of a blowout. The drill pipe passes through the BOP Stack, which consists of the following systems, sub-systems, and components:

- The lower part of the BOP Stack, referred to herein as the BOP, containing five sets of rams: one set of Blind Shear Rams (BSRs), one set of Casing Shear Rams (CSRs), and three sets of Variable Bore Rams (VBRs).
- The upper part of the BOP Stack, referred to herein as the Lower Marine Riser Package (LMRP), contains two annular preventers (Upper Annular [UA] and Lower Annular [LA]).
- Two electronic Control Pods housed on the LMRP. These control pods activate various hydraulic circuits and mechanical components on the BOP Stack.

The LMRP (top) and BOP (bottom), shown in Figure 1, are approximately the height of a six-story building and weigh nearly 400 tons when stacked. In the event of a blowout, various components of the BOP Stack are functioned in an attempt to seal the well. The most important of these components are the BSRs, the large hydraulically actuated rams designed to cut the drill pipe and seal the well. The VBRs, UA, and LA can be used to seal the annular space in the wellbore, however, flow through the drill pipe will continue if these are activated. For the BSRs to contain the DWH blowout, they would have had to operate and completely sever the drill string, allowing the elastomer packers within the rams to contact and seal off the wellbore.

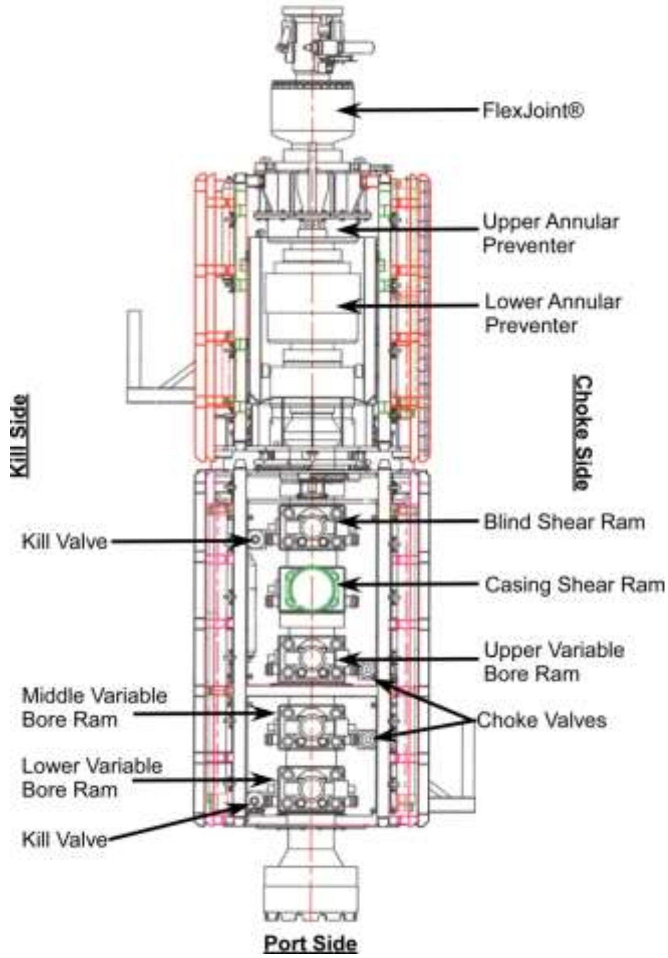

Figure 1. Schematic view of the BOP Stack as viewed from DWH port side

2. Forensic Investigation

2.1 Recovery and Initial Investigation

On September 4, 2010, the BOP Stack was raised from the sea floor. The BOP Stack was transferred by barge to the NASA-Michoud facility in New Orleans, LA. The BSR, CSR, and three sets of VBRs were removed from the lower section of the BOP, cleaned and examined visually and using laser profilometry. The wellbore was examined using high definition video cameras and specific sections were also examined by laser profilometry. The wellbore and the upper and lower annulars in the LMRP were examined using a high definition video camera.

2.2 Drill Pipe Segments

While there was only a single drill pipe present within the wellbore at time of failure, eight (8) drill pipe segments were recovered from various locations during the forensic investigation. Drill pipe segments were recovered from the LMRP, the BOP, and the riser at different stages of the forensic investigation. The segments were matched together using a combination of visual examination of the shear or fracture surfaces, laser profilometry, mechanical and metallurgical testing. A timeline sequence of the various failures in the drill pipe was developed. The final locations of the recovered drill pipe segments indicated that there had been significant movement of the drill pipe during the blowout event. By utilizing the three dimensional (3D) laser scan data, the segments were reconstructed in a computer-aided design (CAD) space to verify pre-failure locations and conditions. The laser scan data was then aligned with the internals scans of the BOP wellbore, and all rams to confirm overall orientations, and eroded flow paths.

2.3 BOP Rams

The BSRs, CSRs, and three sets of VBRs were removed from the lower section of the BOP, cleaned and examined visually and using 3D laser profilometry. The wellbore at the BSRs and annulars in the LMRP were also examined. Based on metallurgical analysis, document review, and digital reconstruction, a timeline of the events leading to the final resting positions of the drill pipe was developed.

Three-dimensional laser scanning provided a means of characterizing surfaces in a quantitative manner and permitted ease of orientation of complex surfaces, as shown in Figure 2. Figure 3 and Figure 4 show that significant erosion occurred on the upper and lower BSR blocks. In order to quantify the erosion damage to the BSR blocks, the laser scan models were compared with design CAD models depicting the nominal geometry for the upper and lower BSR blocks. A contour surface plot of the deviation between the recovered blocks and the CAD model was developed. Figure 3 and Figure 4 show an overlay comparison for the BSR blocks with the laser scan model of the recovered BSR shown as a deviation plot, while the nominal CAD model is overlaid as translucent and outlined. It should be noted there was more damage to the kill side of both the upper and lower BSR than the choke side. The elastomer on the side packers was completely missing and much of the metallic side packer components were eroded away.

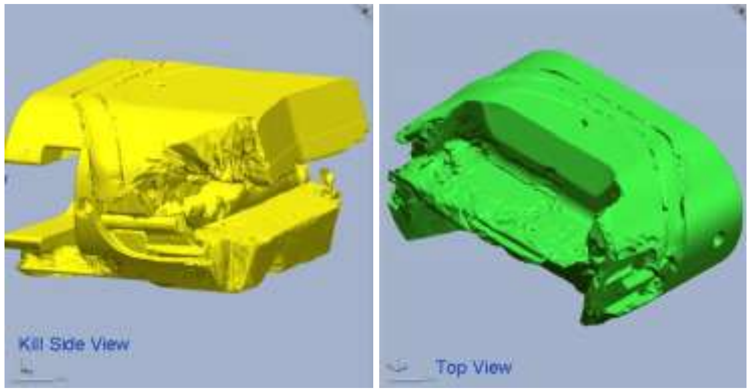

Figure 2. 3D laser scan of Upper (Yellow) and Lower (Green) BSR blocks

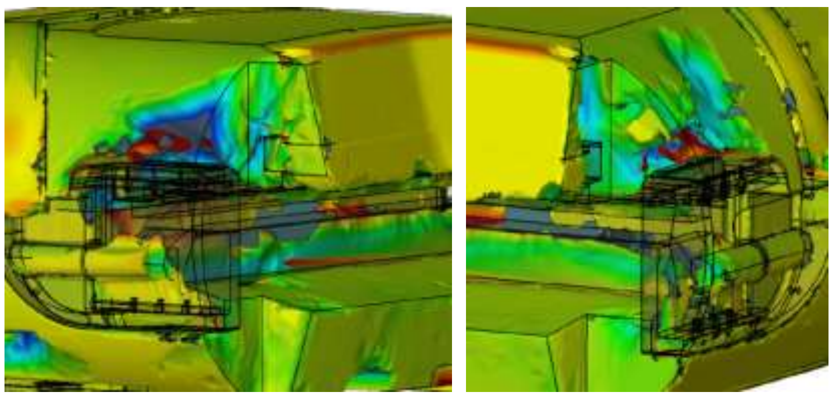

Figure 3. Deviation plots of Upper BSR. (Kill side view on left)

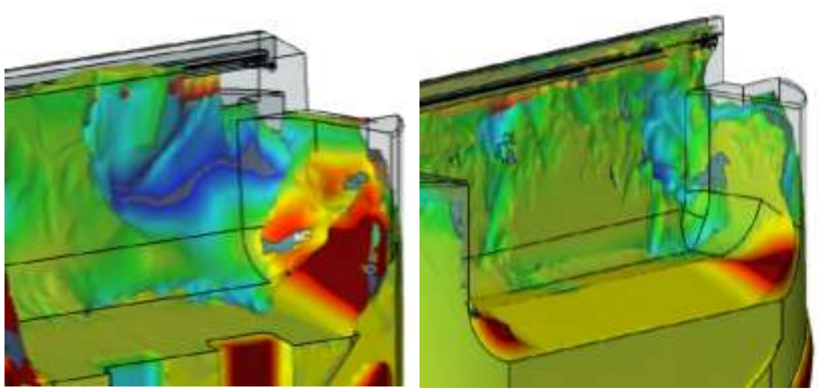

Figure 4. Deviation plots of Lower BSR. (Kill side view on left)

By utilizing the 3D laser scan data, the segments were reconstructed in a computer-aided design (CAD) space to verify pre-failure locations and conditions. The laser scan data was then aligned with the internals scans of the BOP wellbore, and all rams to confirm overall orientations, and eroded flow paths.

Two ends of the recovered drill pipe segments, identified as Pipe Segments 83-B and 94-B in Figure 5 below, were postulated to be partial BSR cuts. This conclusion was based on recovery locations, and visual examination. The physical evidence indicated the drill pipe was out of alignment with design cutting planes of the BSRs. Figure 5 presents the proposed alignment of 3D laser scans of the top and bottom drill pipe segments at the BSR. The features aligned were prominent flat indications and missing corners on the segments cut by the BSR. The aligned features suggest that the drill string was not centered in the well bore at the time of cut. As the BSRs closed, the off centered drill string was positioned such that the corner of the BSR blade prevented the rams from fully shearing the pipe and sealing the well. Theoretically, minor misalignment of the drill pipe should be corrected by the design of the BSR blades, VBRs, and annulars. The digital reconstruction suggested the drill pipe misalignment was not corrected, and it was then necessary to determine why the BOP did not hold the drill pipe centered as designed.

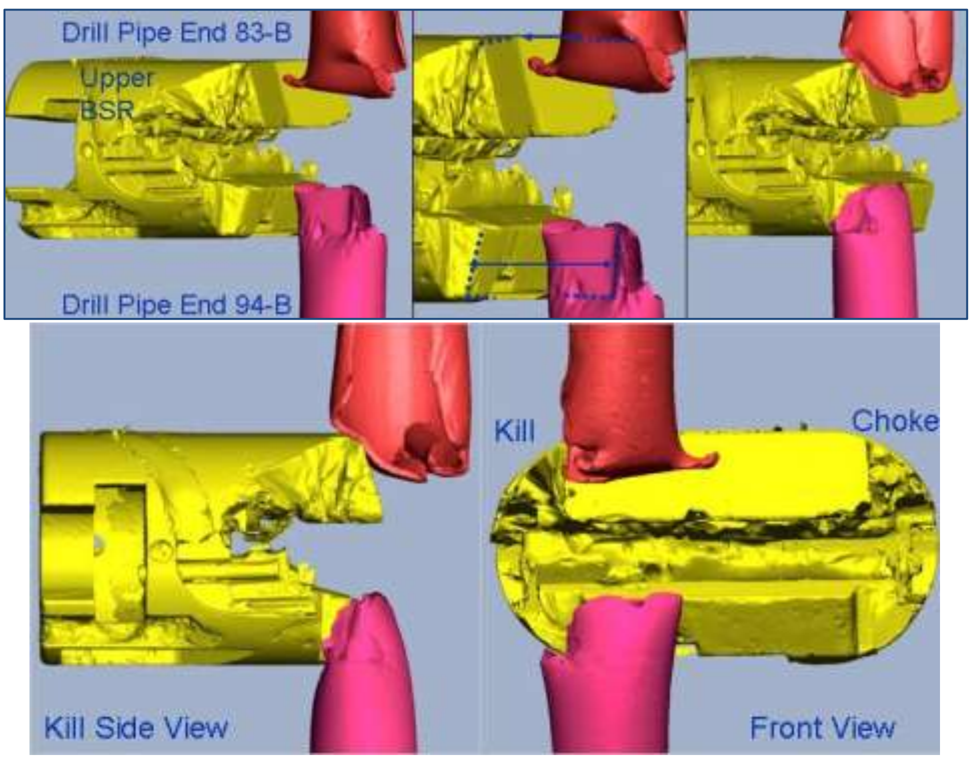

Figure 5. Laser scans of 94-B and 83-B matched against the upper BSR block

3. Modeling

Based on the examination of the damage to the BSR blocks and the drill pipe segments, the position of the drill pipe at the time of cutting by the BSR was not at the center of the wellbore. To explain the position of the drill pipe within the wellbore at the time of the BSR activation, buckling of the drill pipe within the well-bore between the UA and the Upper VBR was examined.

3.1 Buckling Model

Elastic buckling is characterized by a sudden instability of a structure subject to lateral loads or axial compressive loads. In the case of an axially loaded drill pipe, this instability would result in lateral displacement of the pipe within the wellbore. Finite element analysis (FEA) was performed to examine the possibility and effects of elastic buckling of the drill pipe within the wellbore between the UA and the Upper VBR.

The FEA buckle modeling was handled as a two part analysis. A linear eigenvalue buckling analysis was run to predict the likely buckling modes and calculate their corresponding critical loads. A post-buckling Riks analysis was then run utilizing the modified Riks method, to calculate the pipe deformation response after the buckle initiates. The eigenvalue method is a numerical modeling technique to calculate the critical buckling loads of a given structure. For a drill pipe under axial load there are numerous ways in which the drill pipe can buckle (known as buckling modes). The buckling modes are affected by the loading conditions and sensitive to any stiffening elements in the structure. The tool joint and drill pipe were modeled in their entirety for the segment between the UA and the Upper VBR to incorporate any stiffening effects accordingly.

A three dimensional solid model was developed that included a drill pipe segment (including tool joint) that spanned from the UA down to the Upper VBR, the BSR cavity, and a section of the BOP wellbore, as shown in Figure 6. The drill pipe segment was modeled using the nominal geometry specified in API Specification 5D and API Specification 7 (API, 2009). The wellbore and the BSR cavity were modeled to simulate the displacement restrictions of the drill pipe within the wellbore.

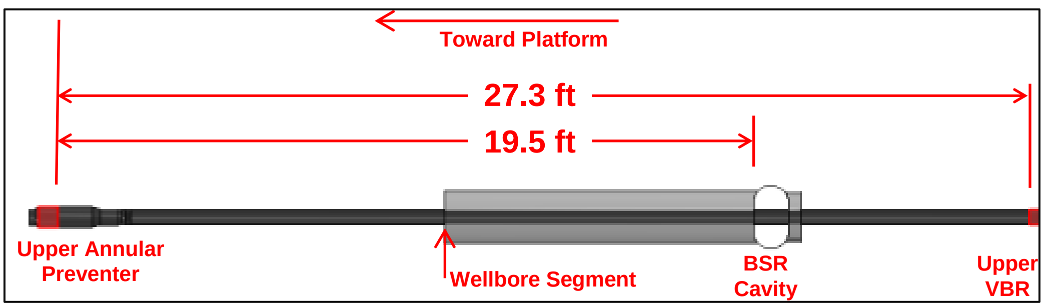

Figure 6. General layout of drill pipe and wellbore section. Note: Graphic orientation is rotated horizontal.

The final drill pipe geometry was modeled with refined mesh of 27,520 elements, connected by 41,400 nodes. The elements used to construct the model were three-dimensional 8-noded hexahedral solid elements. The wellbore and BSR cavity were modeled with rigid shell elements providing contact and displacement control. Elastic material properties were applied to the elements defining the behavior of the drill pipe using results from the mechanical testing of recovered components, as in Table 1 below.

Table 1. Summary of tensile test data for 39-Q

Item ID	Orientation	Diameter	UTS		0.7 YS		Elongation	Reduced Area
		inche	ksi	MPa	ksi	MPa	%	%
39-C	Longitudinal	0.349	160.5	1107	110.6	763	26.0	66.8
39-D	Longitudinal	0.353	160.5	1107	139	958	30.7	68.5
API 5D	Specification	0.350 ± 0.007						
	Minimum	0.343	145	1000	135	931	8.9	
	Maximum	0.357			165	1138		

Boundary conditions were applied representing the constraints at the UA and the Upper VBR. An eigenvalue buckling analysis was then run to predict the buckling modes and calculate their respective critical loads. Critical loads were calculated by applying incremental axial loads to the bottom of the drill pipe until the point of instability was reached. The predicted buckling mode data was then utilized as input for the post-buckling deformation analysis.

The axial load components were added in a static Rik's type analysis to approximate the post-buckling deformation of the drill pipe. Rik's method is capable of varying the applied load components as the pipe deforms allowing the analysis to account for the non-linear effects expected as buckling progresses. The models were solved using Abaqus/Standard. The initial buckling analysis predicted a single waveform buckling mode, at a critical axial load of 113,500 lbs. The predicted deformation and resulting stresses are shown in Figure 7. The predicted deformation showed the peak curvature of the buckle would contact the wellbore slightly above the BSR cavity, holding the pipe against the side of the wellbore.

Having shown it was possible to buckle the pipe at the BSR, it was then necessary to simulate the effects of this off-center scenario. A second FEA study was performed to simulate the ability of the BSR to cut the drill pipe and seal the well with and without the pipe centered in the wellbore.

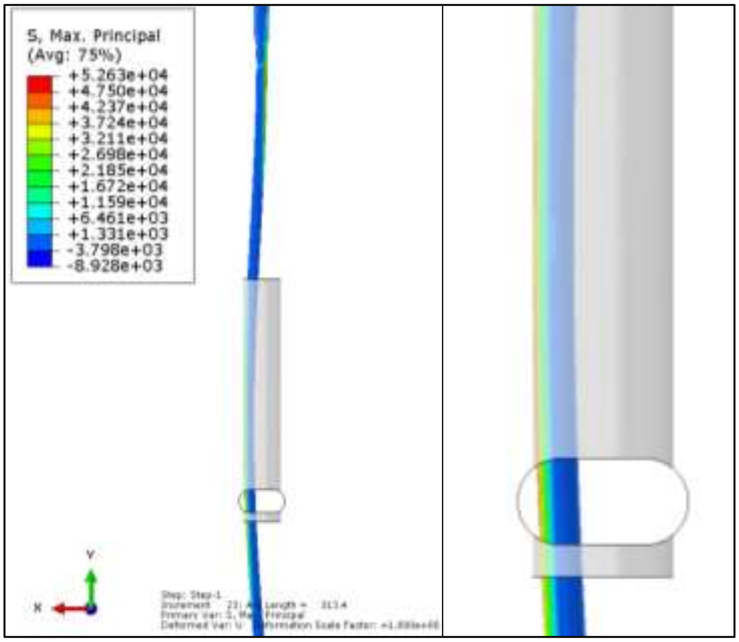

Figure 7. Predicted deformation and resulting stresses due to buckling

3.2 Cutting of the Drill Pipe in the Blind Shear Ram

Physical indications on the ends of Pipe Segments 94-B and 83-B were matched to the outer corners of the upper BSR block as discussed in Section 2.3 above. These indications were aligned with the upper BSR block features to determine the position of the drill pipe within the wellbore. Figure 8 shows a comparison of the aligned pipe segments with the predicted drill pipe position, relative to the BSR cavity, from the buckling analysis.

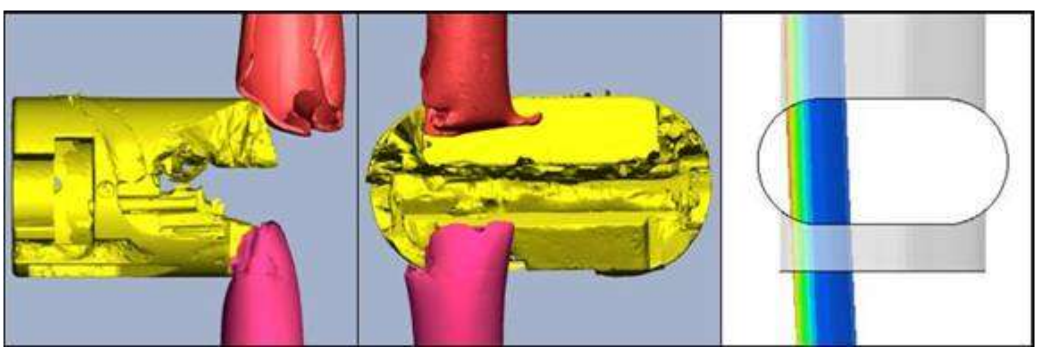

Figure 8. Alignment of pipe segments with BSR and buckled pipe displacement comparison

The BSR blades are designed with a face rake angle intended to impart tension on the drill pipe as the blades shear through it. Multiple numerical equations exist for approximating the shear forces necessary to shear drill pipe, however these only consider situations where the pipe is completely within the shearing blade surfaces of the BSR. A finite element analysis (FEA) was performed to simulate the effects of a non-centered drill pipe on the ability of the BSR to cut the drill pipe and seal the well.

Fracture of a ductile material is governed by two key mechanisms: ductile fracture due to the nucleation, growth, and coalescence of voids (ductile damage) and shear fracture due to shear band localization (shear damage) (Hooputra et al., 2004). These two mechanisms call for different forms of the criteria for the onset of damage. FEA using Abaqus offers several mechanisms to accurately model material damage. For this analysis, ductile damage initiation was specified using the Johnson-Cook damage model and published damage parameters for 4340 steel (Johnson, 1985). The shear damage initiation was specified using shear criterion model within Abaqus/Explicit and published damage parameters. This allowed for the model to consider material failure by ductile damage, shear damage, or a combination thereof.

Validation models were run to determine the forces necessary to cut the drill pipe when it is within the cutting blade surfaces (centered in the wellbore as illustrated in Figure 9). A 3Dshell model was developed representing the BSR blades, block faces, and a section of 5.5 inch diameter drill pipe as shown in Figure 10. The final geometry was modeled with 20,030 elements connected by 20,183 nodes. The blade surface models were developed from CAD models of the BSR provided by manufacturer. The drill pipe was modeled with shell elements and a specified thickness of 0.386 inch, per measurements of Pipe Segment 83. The ram faces were modeled with rigid shell elements as they were assumed stiff relative to the deformable drill pipe. Elastic and plastic material properties were applied to the model defining the behavior of the drill pipe as determined by mechanical testing.

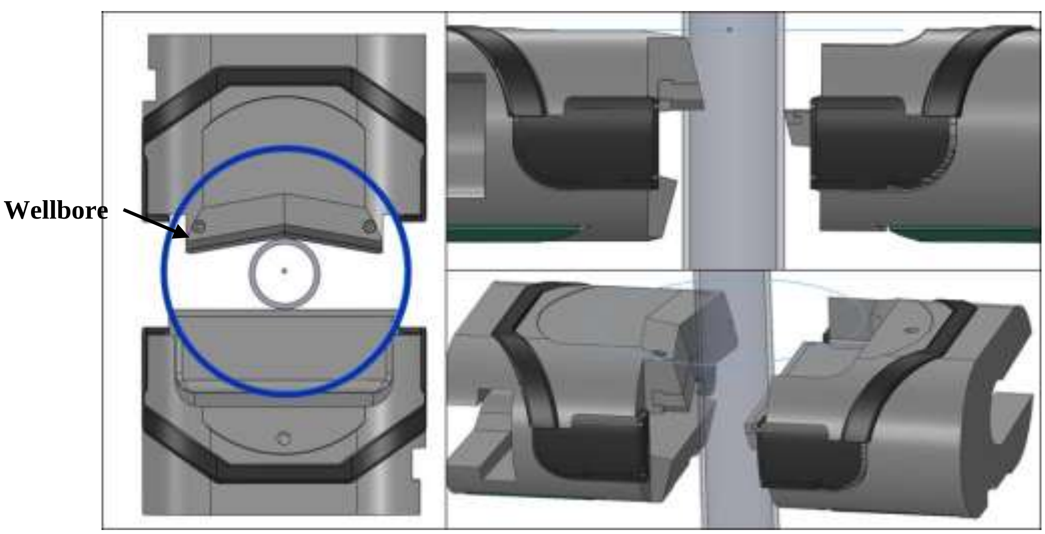

Figure 9. BSR configuration

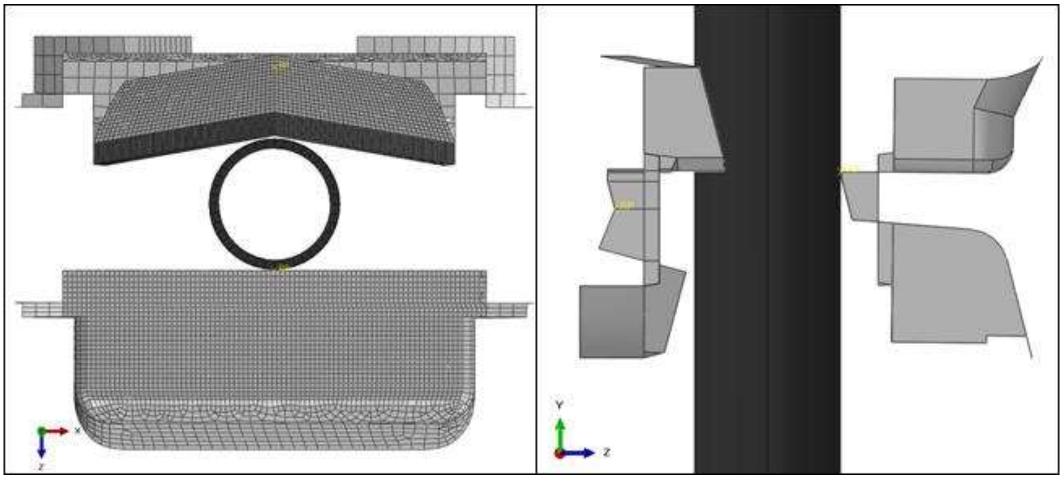

Figure 10. FEA model of BSR blade surfaces and drill pipe

A second model was developed to analyze the effects of the drill pipe being off center in the wellbore (displaced 0.5 inch from the inside wall of the wellbore as illustrated in in Figure 11). The upper BSR block had a single “V” blade design, intended to create a progressive shear, thereby reducing the necessary cutting force. As shown in Figure 9, the upper BSR blade does not extend fully across the wellbore.

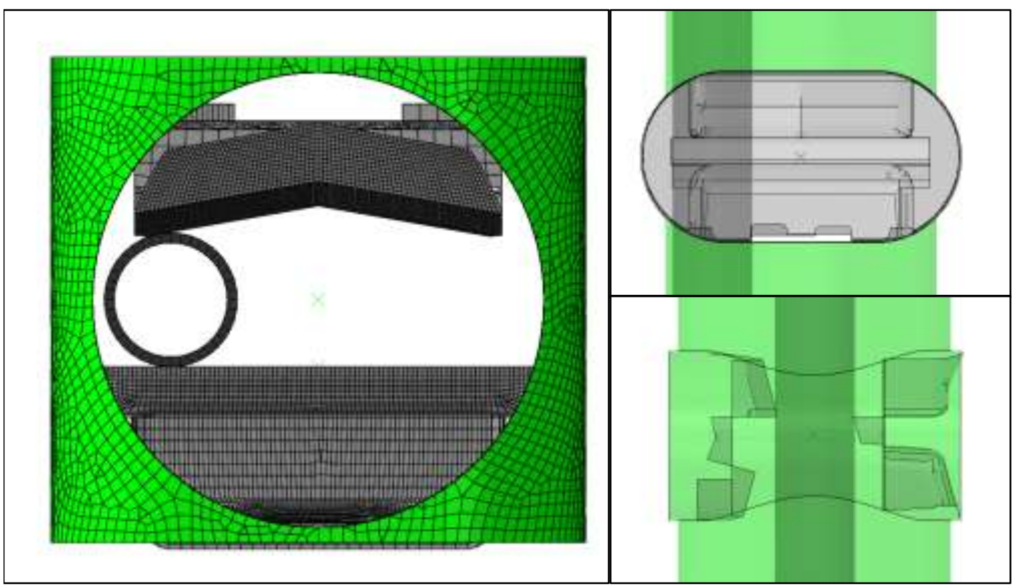

Figure 11. FEA model of BSR blade surfaces and off-center drill pipe

The dynamic pipe shear models were solved using Abaqus/Explicit. The model with centered drill pipe calculated a maximum required shear force of 573,018 lbs. Design details provided the effective piston area for the BSR configuration as 238 in^2. The model-derived shear force, when divided by this effective piston area, equated to a maximum ram pressure of 2,408 psi_g. The FEA results were compared with shearing pressure results derived from multiple empirical methodologies proposed by multiple references, denoted as Method A, B, and C below (Kenney, 2010). Methods A and B below are based on a modified distortion energy theory equation, while Method A utilizes a proprietary empirical formula developed from extensive testing. The calculated results for the given conditions are given in Table 2. The FEA model results showed good agreement with the calculated shear pressures.

Table 2. Comparison of Calculated BSR Pressures

Calculation Method	Calculated Shear Force (lbf_f)	Shear Pressure (psi)
Method A	-	2,378
Method B	504,805	2,121
Method C	-	3,008
FEA Model	573,018	2,408

The BSR is designed to fold the end of the lower pipe segment over to prevent damage to the lateral sealing element behind the upper blade as it passes across. Testing has shown that the lower piece can fracture at the fold point. The centered pipe shear analysis calculated a strain concentration of 32% along the inner bend as seen in Figure 12, matching with the fracture area observed on physical tests.

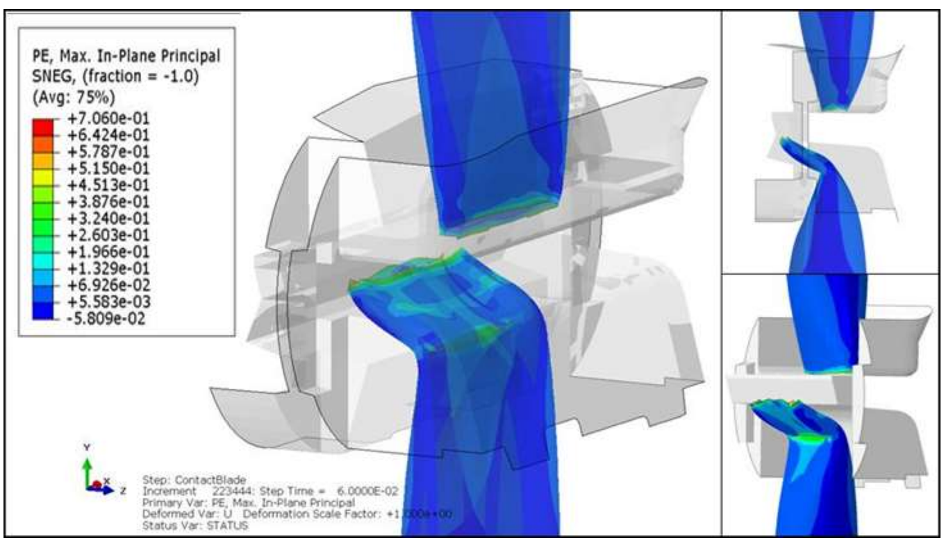

Figure 12. Abaqus FEA model results showing the final deformation of drill pipe at BSR when properly centered.

The off-center shearing analysis demonstrated that with the pipe at the edge of the wellbore, as observed on the recovered drill pipe and predicted by the elastic buckling FEA, the pipe would be deformed outside of the shearing blade. This would have prevented the BSRs from fully shearing and cutting the drill pipe, preventing full closure of the BSRs and sealing of the well. Rather than closing with the sealing surfaces in contact, the drill pipe was deformed and collapsed between the outer faces of the BSRs, outside of the cutting plane, as shown in Figure 13 and Figure 14. The final predicted FEA model simulation was compared with the recovered drill pipe as shown in Figure 15. As shown in the figure, the model of the drill pipe matched well with the indications identified on the recovered forensic evidence.

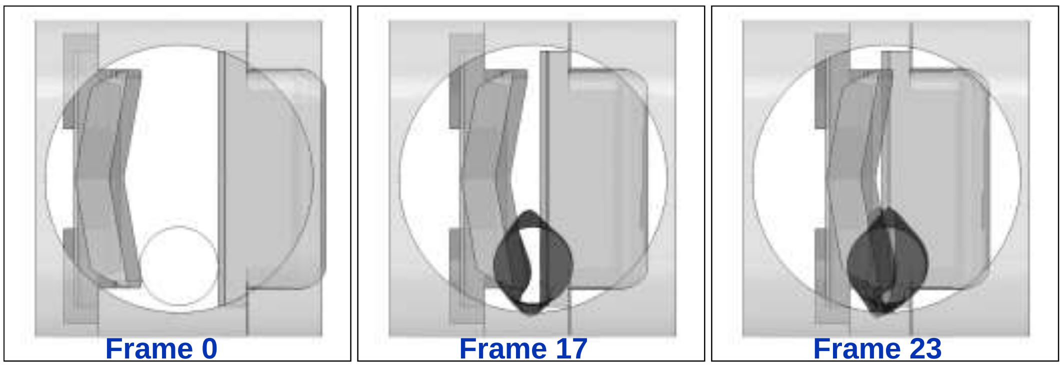

Figure 13. Top View Showing Deformation of Drill Pipe Outside of Shearing Blade Surfaces

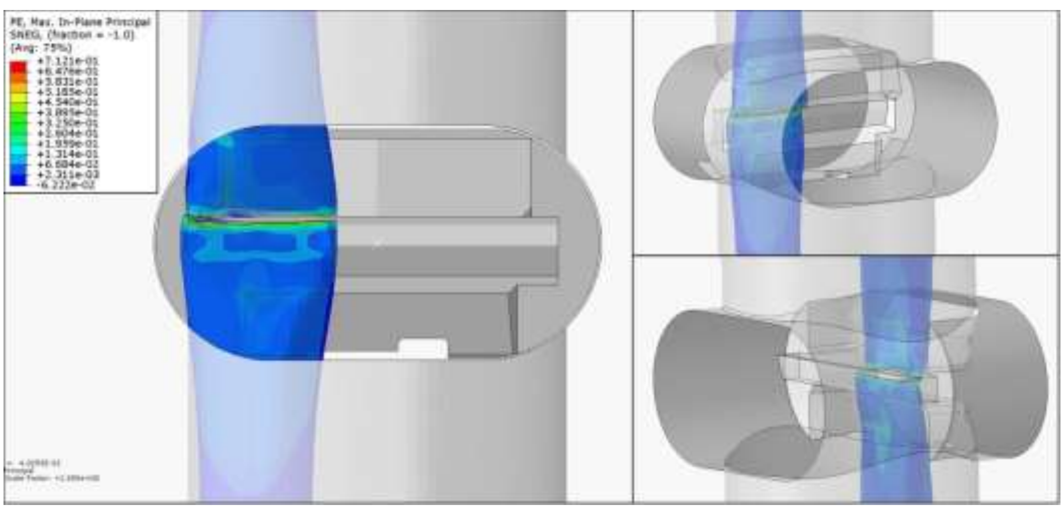

Figure 14. Abaqus FEA model results showing the final deformation of off-center drill pipe at BSR.

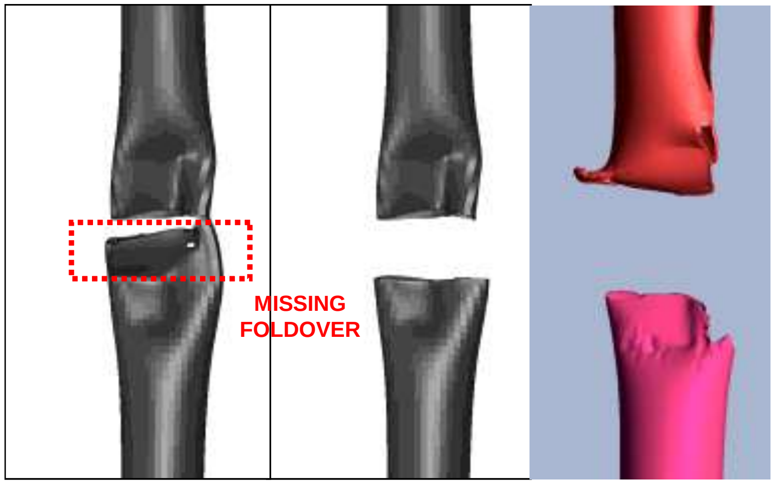

Figure 15. Final model deformation compared with recovered drill pipe laser scans

Based on this shearing model it was possible to calculate an approximate position at which the BSR shear force would exceed capacity of the hydraulic systems; effectively the stall point where the rams could not close further. Per the FEA models analyzed, it was shown that the required shear force exceeded the system capacity, and continued to increase dramatically as the drill pipe compressed between the flats of the ram faces; essentially attempting to crush the pipe steel between flats rather than shearing it. This predicted stall point was reached with the rams approximately 2.8 inch from full closure as shown in Figure 16. Further comparison was performed using the laser scanned models of the recovered shear rams. The models of the upper and lower BSR blocks, and lower drill pipe segment were assembled. With the blocks spaced at the estimated stall point and the lower block fit against Pipe Segment 94 an alternate eroded flow path that could not be sealed even if the BSRs were to fully close at a later point.

The models of the upper and lower BSR were aligned at the predicted 2.8 inch spacing, and the lower BSR fit against the lower drill pipe segment. The predicted configuration at the expected stall point is shown below in Figure 17 showing the significant erosion to the BSR block and packer seals. This prevented the BSR from sealing and allowed for continued flow path through and around the BSR. Erosion to the kill side of the BSRs aligned with the heavy erosion damage on the interior of the wellbore (shown in blue in Figure 17). The extensive erosion on these components created an alternate flow path that could not be sealed even if the BSRs were to fully close at a later point.

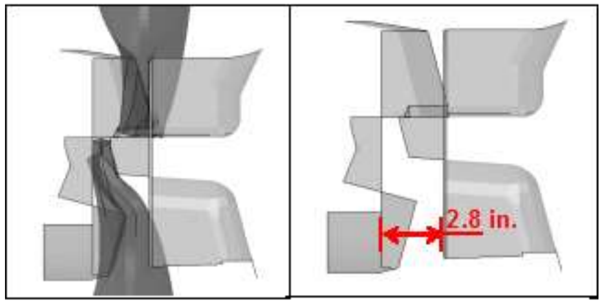

Figure 16. Spacing of upper and lower BSR blocks in partially closed position

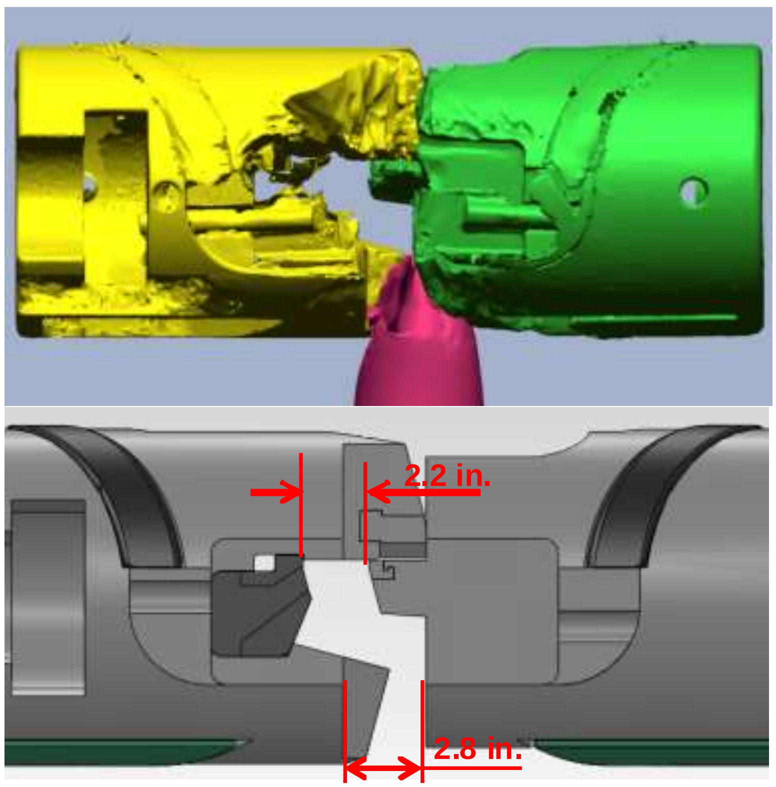

Figure 17. Alignment of scan models and design CAD models showing approximate standoff between BSR faces

4. Primary Cause and Contributing Causes

The forensic investigation identified the primary cause of the blowout event was due to a portion of drill pipe becoming trapped between the BSRs, preventing the BSRs from fully closing and sealing the well.

Contributing causes to the primary cause included:

- The drill pipe elastically buckled within the wellbore due to forces induced on the drill pipe during loss of well control.
- The BSRs were not able to move the pipe cross section into the shearing surfaces of the blades.
- The position of the tool joint at or below the closed Upper Annular prevented upward movement of the drill pipe.
- The Upper VBRs were closed and sealed on the drill pipe.
- The flow of well fluids was uncontrolled from downhole of the Upper VBRs.

5. References

1. Kenney, G.D., Levett, B.A., Thompson, N.G., Bratfos, H., and Bjerager, P., "Forensic Examination of the Deepwater Horizon Blowout Preventer Volume 1," March 2011
2. Kenney, G.D., Levett, B.A., Thompson, N.G., Bratfos, H., and Bjerager, P., "Addendum to Final Report for Forensic Examination of Deepwater Horizon Blowout Preventer," April 2011
3. API Spec 5D, 5thEdition, Specification for Drill Pipe, October 1, 2008
4. API Spec 7, 1st, Specification for Rotary Drill Stem Elements, First Edition, October 1, 2009
5. Hooputra, H., H. Gese, H. Dell, and H. Werner, "A Comprehensive Failure Model for Crashworthiness Simulation of Aluminium Extrusions," International Journal of Crashworthiness, vol. 9, no.5, pp. 449–464, 2004.
6. Johnson, G. R., and W. H. Cook, "Fracture Characteristics of Three Metals Subjected to Various Strains, Strain rates, Temperatures and Pressures," Engineering Fracture Mechanics, vol. 21, no.1, pp. 31–48, 1985.
7. Abaqus Analysis User's Manual, Version 6.11 "21.2.2 Damage Initiation Criteria for Fracture of Metals"; (C) Dassault Systemes, 2010
8. Abaqus Users Manual, Version 6.10-1, Dassault Systémes Simulia Corp., Providence, RI.

6. Acknowledgements

DNV GL would like to acknowledge the DOI for supporting the forensic investigation; Dr. Gary Kenny for his role as technical lead; Captain Sue Englebert (Ret.) of the United States Coast Guard (USCG) for her role in the evidence preservation efforts; NASA's Michoud Assembly Facility and the New Orleans USCG for their hospitality and logistical assistances; and, all DNV staff involved in the forensic investigation.